Journal of Mechanical and Electrical Intelligent System (JMEIS)

Vibration analysis of in-plane bending mode in coupled cylindrical shell using coupled circular ring model for pipe thickness estimation

Takumi Ito[1, a] and Soichiro Takata[2, b,*]

[1]Department of Mechanical Engineering, Kyushu Institute of Technology, 1- Sensui-cho, Tobata-ku, Kitakyushu-shi, 804-8550, Japan

[2]Department of Mechanical Engineering, National Institute of Technology, Tokyo College, 1220-2 Kunugida-machi, Hachioji-shi, 193-0997, Japan

*Corresponding author

[a]< ito.takumi578@mail.kyutech.jp>, [b]<takata@tokyo-ct.ac.jp>

Keywords: vibration diagnosis, continuum vibration, cylindrical shell, coupled circular ring

Abstract. A pipe thickness estimation method using an in-plane bending mode frequency for the detection of the water main deterioration was already proposed in a previous paper. There is a problem that the conventional work was not considered the dependency of the number of connections. The actual distribution mains are consisted by the cylindrical shells of 3m ~ 5m length. However, the behavior of the in-plane bending mode frequency in the gradually increase the number of coupled cylindrical shells is not clear. Moreover, a simplified analysis model is required for conduct the pipe thickness estimation. In this paper, the vibration analysis of in-plane bending mode in coupled cylindrical shell was conducted using a coupled circular ring model for pipe thickness estimation. First, the formulation of analysis model was conducted based on the two-dimensional circular ring model. Furthermore, the vibration experiment was conducted using ideal coupled thin cylindrical shell pipes. In addition, the comparison between experiment result and theoretical result was performed. Finally, the estimation test of pipe thickness was conducted using the experiment results and theoretical model.

1. Introduction

Many distribution pipes for water, gas and oil are deteriorating because of operation beyond their service life. Accidents caused by leaks and bursts result in service interruptions and supply disruptions. Appropriate maintenance is required to prevent accidents. Renewing pipes based on the results of non-destructive testing (NDT) is important for efficient maintenance operations. Therefore, the establishment of NDT technology for in-service pipes is desired in terms of quantification of the deteriorated grade.

NDT technology using the eigen frequency change because of a lack of pipe thickness has been proposed. The method focuses on the in-plane bending vibration mode of the cylindrical shell [1,2,3,4]. The occurrence of the in-plane bending vibration mode in an actual pipe was verified by experiments and numerical simulations [5,6]. Moreover, an analysis of the effects of the incidental structure on the eigen frequency change of the cylindrical shell using the semi-analytical receptance method was conducted to remove the influence of valves, plugs, etc [7]. In addition, an experimental modal analysis was conducted to verify the validation of the above analysis. Furthermore, static deformation analysis using the finite-element method was conducted to determine the correspondence between the vibration test and the actual flattening test [8].

However, the conventional approach does not consider the case of the coupled cylindrical shell. The actual distribution mains consist of coupled cylindrical shells of 3-5m in length. The occurrence of the in-plane bending mode (i.e., ring vibration mode) was confirmed using an experimental modal analysis in a completely coupled actual distribution main as an extreme situation [9].

However, the behavior of the in-plane bending mode frequency in a gradually increasing number of coupled cylindrical shells is not clear. Moreover, a simplified analysis model is required in order to estimate the pipe thickness.

In this study, vibration analysis of the in-plane bending mode in a coupled cylindrical shell was conducted using a coupled circular ring model for pipe thickness estimation. First, the analysis model was formulated based on a two-dimensional circular ring model. The circular rings were coupled with stiffnesses in the radial direction. Furthermore, a vibration experiment was conducted using ideal coupled thin cylindrical shell pipes. Moreover, a comparison between the experiment and theoretical results was conducted. Finally, the pipe thickness was estimated using the experimental results and theoretical model.

2. Formulation of coupled circular ring model

An analysis model based on a coupled circular ring is shown in Fig. 1. The model represents the case when the number of coupled shells is two. Here, only the displacement of the radius direction is assumed. The radius displacement is described as $u_1(\theta), u_2(\theta)$. The under index represents the location of the cylindrical shell. Two shells are connected by a spring along the radial direction, and the spring constant has constant values (i.e., the spring constant is k).

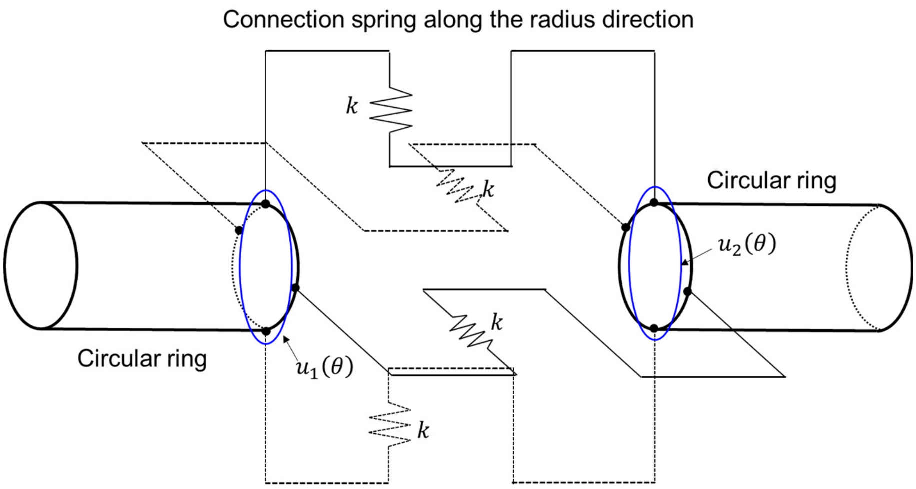

Fig.1. Analysis model of coupled cylindrical shell.

The Lagrangian of Eq. (1) is derived using two-dimensional ring theory.

$$L = \sum_{i=1}^{N} \left\{ \frac{\rho A}{2} \int_0^{2\pi} (\dot{u}_i^2 + \dot{v}_i^2) r d\theta - \frac{EI}{2} \frac{1}{R^3} \int_0^{2\pi} \left(\frac{\partial^2 u_i}{\partial \theta^2} + u_i \right)^2 d\theta \right\} - \sum_{i=1}^{N-1} \left\{ \frac{k}{2} \sum_{l=1}^{M} \left(u_i(\theta_l) - u_{i+1}(\theta_l) \right)^2 \right\} \tag{1}$$

Here, u_i represents the displacement in the radius direction, v_i represents the displacement in the circumference direction, $\dot{u}_i$ represents the velocity in the radius direction, $\dot{v}_i$ represents the velocity in the circumference direction, N represents the number of circular rings, M represents the number of springs along the radial direction, L represents the length of the cylindrical shell, h represents the pipe thickness, R represents the average radius, E represents Young's modulus, ρ represents the density, A represents the sectional area ($A = Lh$), and I represents the moment of inertia of area ($I = Lh^3/12$). Here, the geometrical conditions are supposed as follows: $L/R \geq 2$ and $R/h \gg 1$ [10].

The displacement in the radius direction is as follows:

$$u_i = a_i \cos 2\theta + b_i \sin 2\theta . \tag{2}$$

Here, it is assumed that circumferential wave number is 2; moreover, a_i, b_i represent the generalized coordinates.

For example, the calculation result of the equation of motion is as follows, using the Lagrangian equation when the number of connections is 2:

$$\begin{cases} M\ddot{a}_1 + Ka_1 + k_{cc}(a_1 - a_2) + k_{cs}(b_1 - b_2) = 0 \\ M\ddot{b}_1 + Kb_1 + k_{cs}(a_1 - a_2) + k_{ss}(b_1 - b_2) = 0 \\ M\ddot{a}_2 + Ka_2 + k_{cc}(a_2 - a_1) + k_{cs}(b_2 - b_1) = 0 \\ M\ddot{b}_2 + Kb_2 + k_{cs}(a_2 - a_1) + k_{ss}(b_2 - b_1) = 0 \end{cases} . \tag{3}$$

The equivalent mass, equivalent spring constant, and coupled spring constant are as follows:

$$M = \frac{5}{4}\pi\rho AR, K = \frac{9EI}{R^3}\pi, \tag{4}$$

$$\begin{cases} k_{cc} = k\left(\sum_{l=1}^{M} \cos^2\left[2\frac{2\pi}{M}(l-1)\right]\right) \\ k_{cs} = k\left(\sum_{l=1}^{M} \cos\left[2\frac{2\pi}{M}(l-1)\right]\sin\left[2\frac{2\pi}{M}(l-1)\right]\right) \\ k_{ss} = k\left(\sum_{l=1}^{M} \sin^2\left[2\frac{2\pi}{M}(l-1)\right]\right) \end{cases} . \tag{5}$$

3. Experimental setup

3.1 Test pipe

The coupled circular ring was composed of a general aluminum cylindrical shell. The parameters of the cylindrical shell were as follows: thickness $h = 0.11$ mm, length $L = 127$ mm, and radius $R = 32.5$ mm. The circular rings were connected using an aluminum tape (thickness of 0.1 mm), as shown in Fig. 2. The aluminum tape had notches in the circumferential direction. The bending mode wave of the long wavelength did not affect the notches because the spaces between notches differed from the wavelength of the second in-plane bending mode. Here, the wavelength of the second in-plane bending mode was 102.1 mm, and the spaces between notches were approximately 2.9 mm (i.e., $M = 70$). A schematic of the connection method is presented in Fig. 3. The aluminum tape had no cut region (approximately 1 mm) in the center of width. The synchronized motion between the edges of the two circular rings was realized by the contribution of no region motion. Here, the number of connections was 2 (total length $L = 258$ mm) and 8 (total length $L = 1033$ mm).

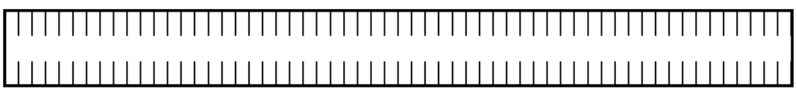

Fig. 2. Schematic figure of aluminum tape to connect the circular rings. The schematic is view from above. Here, the black stripes represent the notch.

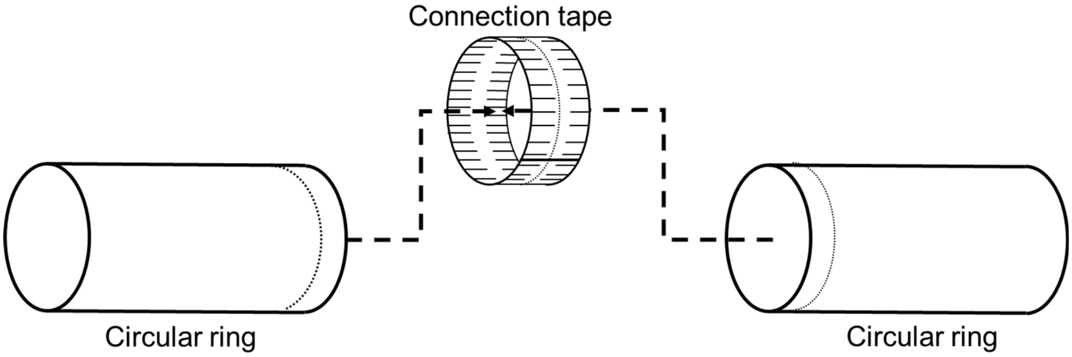

Fig. 3. Connection arrangement of coupled thin circular rings.

3.2 Experimental setup

A schematic diagram of the experimental setup is shown in Fig. 4. The exciter was WaveMaker05 (Asahi Seisakusyo, Inc.), and the power amplifier was APD-050FCA (Asahi Seisakusyo, Inc.) and the fast Fourier transform (FFT) analyzer was DS-2000 (Ono Sokki, Inc.). The output signal of the swept sine wave was generated by the function of the FFT analyzer. The excitation force was loaded in the center of the coupled cylindrical shell, and the acceleration sensor was placed in the upper part of the shell. The acceleration signal was input to the FFT analyzer. The frequency response function was obtained using the cross-spectrum between the input and output signals. The condition of signal measurement was as follows. The sampling frequency was 2 kHz, the voltage range was 1.41 V, the number of samples for FFT was 4096, and the average of the frequency response function was conducted from 100 measurements.

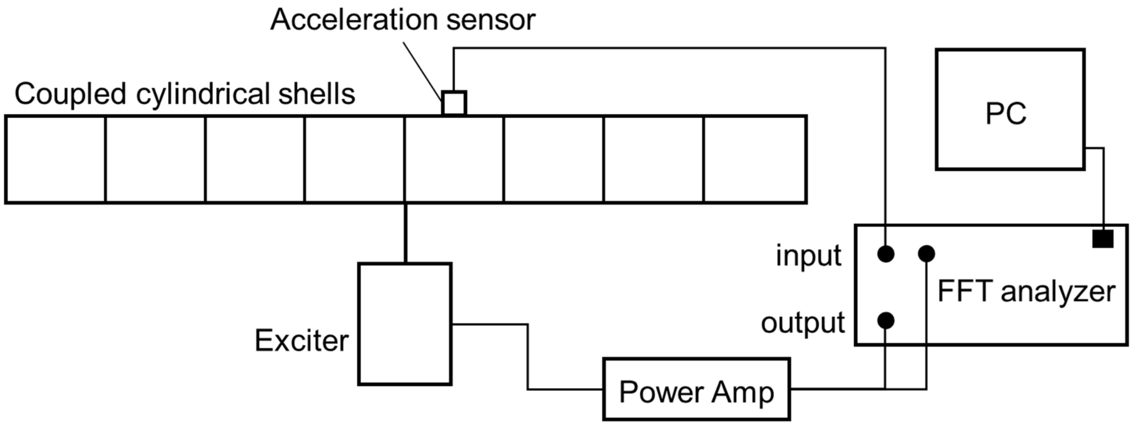

Fig. 4. Experimental setup: the system contains the FFT analyzer, acceleration sensor, power amplifier, exciter, and coupled cylindrical shell. The coupled cylindrical shell is suspended by thin strings. Furthermore, exciter is excited by sweep signal from FFT analyzer.

4. Results and discussion

The experimental values of the frequency response function are shown in Fig. 5. The horizontal axis represents the frequency, and the vertical axis represents the amplitude. Furthermore, the black solid line shows the case where the number of connections is two, and the blue solid line shows the case where the number of connections is eight. The resonance peaks in the case of two connections can be observed a 71.9 and 103 Hz. Similarly, the resonance peaks in the case of eight connections are found at 65, 76, 85 and 102 Hz. The above experimental values are indicated by the black and blue dotted lines in Fig. 5.

Furthermore, experimental and calculation results were compared using the theoretical model in the Chapter 2. The calculation conditions are as follows: Young's modulus $E = 86\ \mathrm{GPa}$, density $\rho = 2800\ \mathrm{kg/m^3}$, pipe length $L = 127\ \mathrm{mm}$, pipe thickness $h = 0.11\ \mathrm{mm}$, and average radius $R = 32.5\ \mathrm{mm}$. When the number of connections is two, the spring constant k is chosen to agree with the calculation and experimental values; as a result, the spring constant k is 20 N/m. The number of springs in circumferential direction (M) is 70.

The results of the experiment and calculation values for the number of connections are listed in Table. 1. The two observable modes are obtained by considering the node in the mode shape, and the calculated eigenfrequencies are 63.3 and 105.4 Hz, respectively. On the other hand, the experimental values are 71.9 and 102.0 Hz, and the errors are 13.5% and 3.3%, respectively. The lower calculated eigenfrequency of 63.3 Hz agrees with the theoretical value of the two-dimensional circular ring [11]. The coupled spring constant is not contributed to lowest frequency because of the two rings are displace in same radius direction, as the result, the lowest frequency of the connected rings agrees with the two-dimensional ring without connection.

The ring frequency is as follows:

$$\omega_n = \frac{n(n^2-1)}{\sqrt{n^2+1}}\frac{1}{R^2}\sqrt{\frac{EI}{\rho A}}, I = \frac{Lh^3}{12}, A = Lh \tag{6}$$

The results of the experiment and calculation values in the case where the number of connections is eight are shown in Table. 2. The four observable modes are obtained considering the node in mode shape, and the calculated eigenfrequencies are 63.3, 78.0, 91.6, and 105.4 Hz. On the other hand, the experimental values are 65.0, 76.0, 85.0, and 102.0 Hz, and the errors are 2.7%, 2.6%, 7.2%, and 3.3%, respectively. The lower calculated eigenfrequency (63.3 Hz) also agrees with the theoretical value of the two-dimensional circular ring.

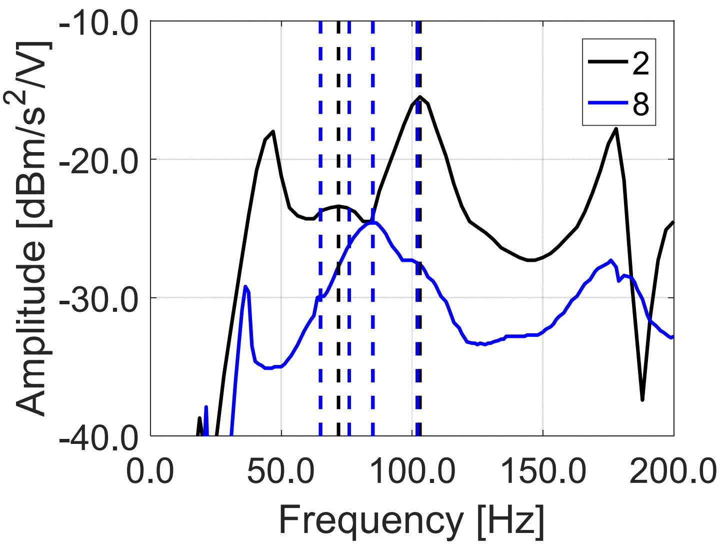

Fig. 5. Frequency response function when the numbers of connections are two and eight. Here, black dotted lines show the eigenfrequency in case of the number of connections of two, blue dotted lines show the eigenfrequency in case of the number of connections of eight.

Table 1 Summary of experimental and calculation results when the number of connections is two

Experiment value	Calculation value	Mode shape
71.9Hz	63.3Hz	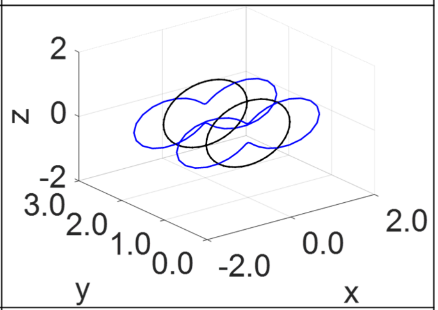
Un-observable mode due to node position	63.3Hz	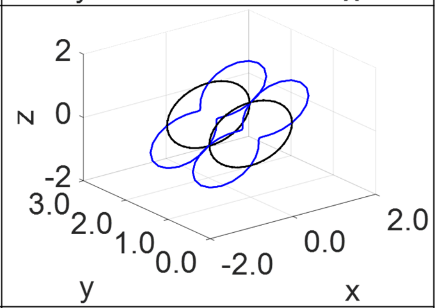
102.0Hz	105.4Hz	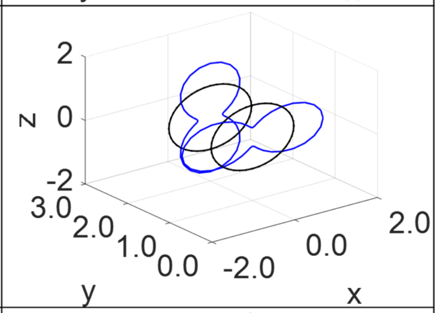
Un-observable mode due to node position	105.4Hz	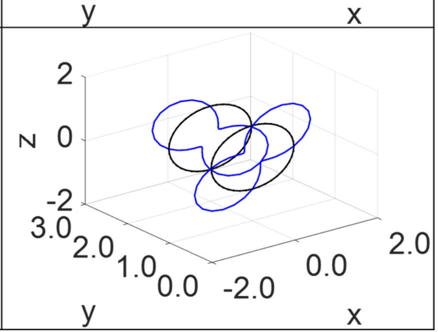

Table 2 Summary of experimental and calculation results when the number of the connections is eight

Experiment value	Calculation value	Mode shape
65.0Hz	63.3Hz	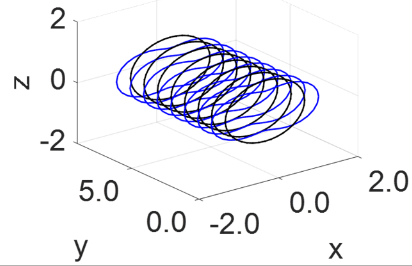
Un-observable mode due to node position	63.3Hz	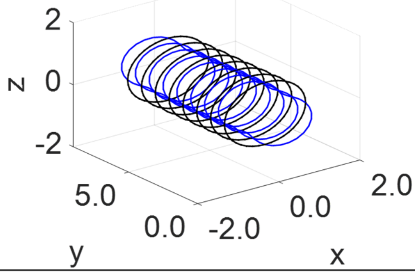
Un-observable mode due to node position	67.4Hz	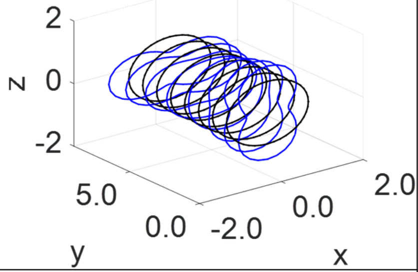
Un-observable mode due to node position	67.4Hz	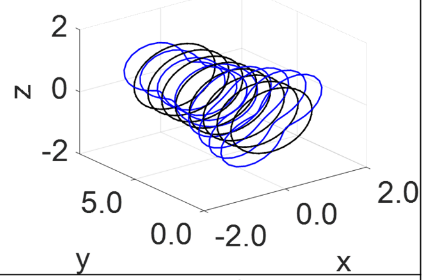
76.0Hz	78.0Hz	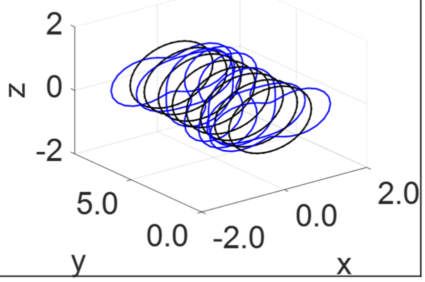

Table 2 Summary of experimental and calculation results when the number of the connections is eight (continued)

Experiment value	Calculation value	Mode shape
Un-observable mode due to node position	78.0Hz	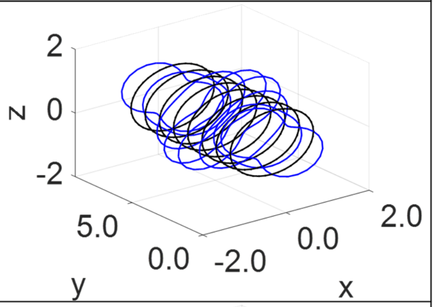
85.0Hz	91.6Hz	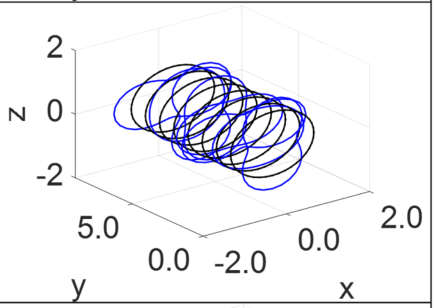
Un-observable mode due to node position	91.6Hz	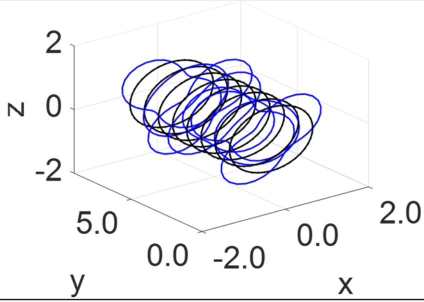
102.0Hz	105.4Hz	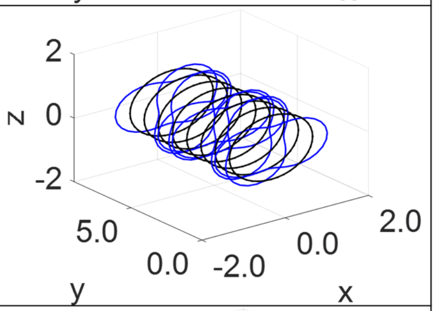
Un-observable mode due to node position	105.4Hz	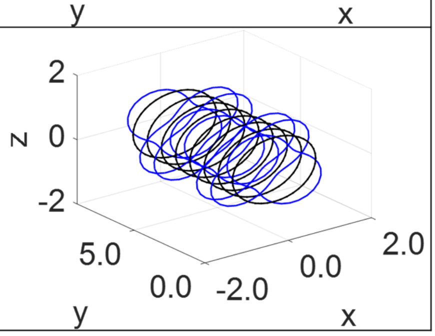

5. Application to pipe thickness estimation using the inverse analysis of eigen frequency

Pipe thickness estimation was conducted using an inverse analysis based on two-dimensional ring theory. The inverse problem for pipe thickness estimation is defined by Eq. (7).

$$h^* = \underset{h}{\operatorname{argmin}} J = \underset{h}{\operatorname{argmin}} \left| f_{\mathrm{exp}} - g(E, \rho, v, L, R, h, n) \right|^2 \tag{7}$$

The estimated pipe thickness was obtained by minimizing the objective function J of Eq. (7). Here, the function g was selected as suitable for the experimental values and theoretical prediction model. For example, in the case of the ring resonance frequency, the function g was given by Eq. (6). The method based only a lowest frequency is verified the simplest case in this paper. The authors will consider the case of the estimation using the multiple eigen frequencies in the future work.

The visualization results of the objective function shape are shown in Fig. 6 for the ring resonance frequency. The horizontal axis represents the estimated pipe thickness, and the vertical axis represents the value of the objective function. In addition, the different colors of the solid line show the various cases based on the experimental eigenfrequencies (see Table 3). The eigenfrequencies contain the reading error of eigenfrequency from peak of frequency response function.

The calculation conditions are as follows: Young's modulus $E = 86$ GPa, Poisson's ratio $v = 0.345$, density $\rho = 2800\ \mathrm{kg/m^3}$, average radius $R = 32.5$ mm, and wavenumber of the circumferential direction $n = 2$. As a result, the objective function shape is a valley structure. The trends were observed for different experimental eigen frequencies. Therefore, the estimated pipe thickness was obtained by referring to the thickness at the minimum value of the objective function.

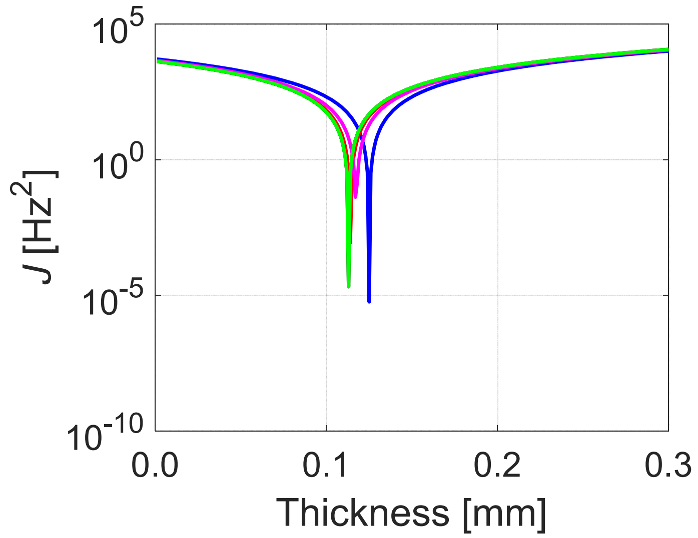

Fig.6. Visualization result of the objective function to estimate the pipe thickness. Here, blue solid line shows the case of the number of connections of 2, red solid line shows the case of the number of connections of 4, magenta solid line shows the case of the number of connections of 6, green solid line shows the case of the number of connections of 8.

The estimation results for the pipe thickness are represented in Table 3. The estimated thicknesses were obtained in the range of 0.113-0.125 mm. However, the true value of the pipe thickness was 0.11 mm; hence, the relative error between true and estimation ranged from 2.73% to 13.6%. Thus, the realization of pipe thickness estimation using the eigenfrequency of the in-plane bending vibration mode is implied. In future work, confirmation of the actual field distribution is expected using the proposed diagnosis method.

Table 3 Estimation results of the pipe thickness.

Number of connections	Estimation result	
	Frequency [Hz]	Thickness [mm]
1	65.0	0.113
2	71.9	0.125
4	65.6	0.114
6	67.5	0.117
8	65.0	0.113

6. Conclusions

In this study, the vibration analysis of the in-plane bending mode was performed using a coupled circular ring model. Moreover, the pipe thickness estimation based on the eigen frequency of the in-plane bending vibration mode was performed. The following results were obtained.

(1) The analysis model was formulated using a coupled ring model with spring stiffness along the radial direction. In addition, the model was verified comparing the experimental and theoretical consideration.

(2) The lowest eigenfrequency of the above analysis model agreed with the two-dimensional ring frequency.

(3) The pipe thickness estimation was verified operationally. The error between the true and estimation values ranged from 2.73% to 13.6%.

Acknowledgments

This work was supported by JSPS KAKENHI Grant Number JP20K14685.

References

[1] J. P. Den Hartog, "Mechanical vibrations", ***Dover Publications,*** p.165-p.169, 1985.

[2] W. Flugge, "Statik and dynamic der schalen 3rd ed", ***Springer,*** 1962.

[3] A. H. E. Love, "The mathematical theory of elasticity 4th ed", ***Macmillan,*** 1959.

[4] W. Soedel, "Vibration of shells and plates", ***CRC Press,*** 2004.

[5] H. Inoue, S. Takata and S. Shinoda, "Simplified description of in-plane bending mode of cylindrical shell using two-dimensional ring model", ***Symposium on Evaluation and Diagnosis 16,*** 109, 2017 (in Japanese).

[6] S. Shinoda, H. Inoue and S. Takata, "Thinning pipe wall detection using coupled oscillation between cylindrical shell and attached sub-structure", ***Symposium on Evaluation and Diagnosis 16,*** 104, 2017 (in Japanese).

[7] S. Takata, H. Inoue and S. Shinoda, "Vibration analysis of cylindrical shell with sub-structure using Semi-Analytical Receptance Method", ***Symposium on Evaluation and Diagnosis 16,*** 108, 2017 (in Japanese).

[8] H. Inoue and S. Takata, "Investigation on the equivalent parameters of in-plane bending vibration in cylindrical shell using finite element method", ***Symposium on Evaluation and Diagnosis 17,*** 210, 2018 (in Japanese).

[9] S. Takata, H. Inoue and S. Shinoda, "Proposal of the pipe diagnosis method using in-plane bending vibration of cylindrical shell", ***Transactions of the Japan Society of Mechanical Engineers,*** Vol.84, No.861, DOI:10.1299/transjsme.17-00522, 2018 (in Japanese).

[10] Koga, T, "The minimum natural frequencies and vibration characteristics of circular cylindrical shells", ***Transactions of the Japan Society of Mechanical Engineers, Series A,*** Vol.46, No.411, pp.1280–1289, 1980 (in Japanese).

[11] S. P. Timoshenko and I. Tanishita, "Vibration problem in engineering", ***Tokyo tosho,*** 1981 (in Japanese).